Journal of the European Ceramic Society **14** (1994) 455–462

The Effect of Boria and Titania Addition on the Crystallization and Sintering Behavior of Li_2O–Al_2O_3–$4SiO_2$ Glass

Yun-Mo Sung,*[a] Stanley A. Dunn[b] & James A. Koutsky[b,c]

[a] Department of Material Science and Engineering, [b] Department of Chemical Engineering, and [c] Materials Science Program, University of Wisconsin–Madison, Madison, Wisconsin 53706, USA

(Received 1 November 1993; revised version received 8 April 1994; accepted 27 May 1994)

Abstract

Crystallization and sintering behaviors of four β-spodumene (Li_2O–Al_2O_3–$4SiO_2$) glasses having different compositions were investigated and compared by differential thermal analysis (DTA), X-ray diffraction (XRD), and scanning electron microscopy (SEM). The Li_2O–Al_2O_3–$4SiO_2$ glass containing both B_2O_3 and TiO_2 showed the lowest activation energy value for crystallization (220 ± 8 kJ/mol), whereas the stoichiometric Li_2O–Al_2O_3–$4SiO_2$ glass showed the highest value (322 ± 4 kJ/mol). The crystallization peak temperature (T_p) decreased from 918 to 819°C by the addition of both B_2O_3 and TiO_2 to the stoichiometric Li_2O–Al_2O_3–$4SiO_2$ glass. The Li_2O–Al_2O_3–$4SiO_2$ glass containing both B_2O_3 and TiO_2 showed approximately the same degree of sintering as the Li_2O–Al_2O_3–$4SiO_2$ glass containing only B_2O_3.

Die Kristallisation und das Sinterverhalten von vier β-Spodumengläsern (Li_2O–Al_2O_3–$4SiO_2$) mit verschiedener Zusammensetzung wurden mittels Differentialthermoanalyse (DTA), Röntgenbeugung (XRD) und Rasterelektronenmikroskopie (SEM) untersucht und verglichen. Das Li_2O–Al_2O_3–$4SiO_2$-Glas, das sowohl B_2O_3 als auch TiO_2 enthielt, hatte die niedrigste Aktivierungsenergie für die Kristallisation (220 ± 8 kJ/mol), wohingegen das stöchiometrische Li_2O–Al_2O_3–$4SiO_2$-Glas den höchsten Wert aufwies (322 ± 4 kJ/mol). Der Höchstwert der Kristallisationstemperatur (T_p) für stöchiometrisches Li_2O–Al_2O_3–$4SiO_2$-Glas fiel bei Zugabe von B_2O_3 und TiO_2 von 918 auf 819°C. Das Li_2O–Al_2O_3–$4SiO_2$-Glas, das sowohl B_2O_3 als auch TiO_2 enthielt, wies in etwa den selben Sinterungsgrad auf als Li_2O–Al_2O_3–$4SiO_2$-Glas, das nur B_2O_3 enthielt.

Le comportement au frittage et à la cristallisation de quatre verres de type β-spodumene (Li_2O–Al_2O_3–$4SiO_2$) présentant différentes compositions ont été étudiés et comparés par analyse thermique différentielle (DTA), diffraction de rayons X (XRD) et microscopie électronique à balayage (JEM). Le verre Li_2O–Al_2O_3–$4SiO_2$ contenant à la fois du B_2O_3 et du TiO_2 présente l'énergie d'activation relative à la cristallisation la plus faible (220 ± 8 kJ/mol), alors que le verre Li_2O–Al_2O_3–$4SiO_2$ stoechiométrique se caractérise par la valeur la plus élevée (322 ± 4 kJ/mol). La température (T_p) à laquelle le pic de cristallisation est observé diminue de 918 à 819°C, suite à l'addition conjointe du B_2O_3 et du TiO_2 au verre Li_2O–Al_2O_3–$4SiO_2$ stoechiométrique. Le verre Li_2O–Al_2O_3–$4SiO_2$ avec ajout de B_2O_3 et TiO_2 montre approximativement la même aptitude au frittage que le verre Li_2O–Al_2O_3–$4SiO_2$ contenant uniquement du B_2O_3.

1 Introduction

Glass-ceramics are crystalline materials which can be formed by controlled crystallization heat treatments of proper glasses. Most of them have some unique properties such as translucency, high strength, and very low and uniform thermal expansion. They also have very fine (~1 μm) and randomly oriented crystals with a few percent of the residual glass.[1] The recent applications of glass-ceramics are for matrix materials for ceramic fiber-reinforced composite materials,[2–6] substrate materials for semiconductor packaging,[7–8] heat exchangers,[1] telescope mirrors[9] and cooking wares.[10]

A relatively new method of glass-ceramic preparation is the sintering of glass powders, followed by a nucleation heat treatment.[11–15] This technique

* To whom correspondence should be addressed.

gives cost benefits by reducing the processing temperatures. Furthermore, the formation of complex shapes can be obtained by using equipment common to a ceramic factory.[11]

β-Spodumene (Li_2O–Al_2O_3–$4SiO_2$) is a glass-ceramic well-known for its good mechanical properties (strength of ~150 MPa and modulus of ~100 GPa) and extremely low thermal expansion (thermal coefficient of expansion of $\sim 9 \times 10^{-7}$/°C).[16]

The introduction of TiO_2 as a nucleating agent in Li_2O–Al_2O_3–SiO_2 systems has been reported to lead to titanate formation and phase separation. Barry *et al.*[17] reported the formation of precursor nuclei of small crystallites, consisting of a titanium-containing compound in the heat-treated Li_2O–Al_2O_3–SiO_2 glasses. Doherty *et al.*[18] reported that $Al_2Ti_2O_7$ crystals were precipitated and that these crystals act as nuclei for crystallization in a Li_2O–Al_2O_3–SiO_2–TiO_2 system. Maier & Muller[19] reported the formation of $ZrTiO_4$ crystallites which also act as the precursor nuclei for subsequent crystallization in Li_2O–Al_2O_3–SiO_2–TiO_2–ZrO_2 system. Recently Hsu & Speyer[20] observed that the introduction of TiO_2 and Ta_2O_5 in the Li_2O–Al_2O_3–$6SiO_2$ system promoted nucleation and crystal growth in the bulk glasses by causing the precipitation of crystalline precursor phases which are dispersed within the phase separated glass, and which acted as heterogeneous nucleation sites for the formation of a β-quartz solid solution.

Buzhinskii *et al.*[21] reported that in the heating of the Li_2O–Al_2O_3–SiO_2–TiO_2 glasses, segregation into two drop-like glassy phases occurs, resulting in an increased viscosity of the glass. The size of the drops decreases with decreasing heat-treatment temperature; however, their number increases. Only after the two phases are separated does a rearrangement of the structure occur within the new phase, with the formation of a crystalline lattice. Kondrat'ev and coworkers[22] investigated the crystallization of glasses of the Li_2O–Al_2O_3–SiO_2 system and also observed the formation of liquids of Al_2O_3–TiO_2 type already in the melt, which can serve as nuclei. Beall & Duke[1] indicated that the addition of cations such as Ti^{4+}, Zr^{4+}, Hf^{4+}, Nb^{5+}, Mo^{6+}, W^{6+} and Cr^{3+} can cause the homogeneous glass melt to become immiscible. They observed the amorphous phase separation that develops on cooling of Li_2O–Al_2O_3–SiO_2–TiO_2 glass by transmission electron microscopy (TEM).

The conventional glass-ceramic technology is based on glasses that result in heterogeneous bulk crystallization. The crystallization takes place at high viscosities, preventing significant deformation of glass bodies. If this kind of glass is finely ground and compacted again, every particle will crystallize separately, resulting in a dramatic increase in viscosity.[14] Therefore, good sintering and high strength sintered bodies can not be obtained using this method. Rabinovich[14] showed that glasses which are usually capable of surface crystallization at relatively low viscosities may be successfully sintered. Although every particle crystallizes from its surface, the significant surface area of ground material ensures a fine crystallization similar to that in bulk glass-ceramics with heterogeneous nucleation. Rabinovich[14] examined about 40 glasses based on the composition of cordierite ($2MgO$–$2Al_2O_3$–$5SiO_2$). All of the glasses with TiO_2 as a nucleating agent crystallized prematurely and showed poor sintering except those glasses containing Na_2O. Cordierite with 4·5 wt% P_2O_5 showed the highest shrinkages during sintering. Giess *et al.*[13] made cordierites with the glass formers such as B_2O_3 and P_2O_5. They studied the sintering process of pressed pellets and found pronounced anisotropy of shrinkage as a result of uniaxial pressing. They found that Frenkel's theory of sintering gives a good approximation only to the initial stages of sintering. Recently Knickerbocker *et al.*[15] studied the effect of various oxide additions on the sintering behavior of β-spodumene (Li_2O–Al_2O_3–$4SiO_2$) glass-ceramics. They reported that the addition of 3 wt% B_2O_3 or P_2O_5 to the stoichiometric β-spodumene glass-ceramic can enhance sintering. By addition of 3 wt% of P_2O_5 and B_2O_3 the shrinkage of the glass pellets during sintering increased by 4·2% and 0·5%, respectively. Also, Knickerbocker *et al.*[8] studied the sintering of cordierite glass-ceramic with B_2O_3 and P_2O_5 addition. In both papers they mentioned that to obtain good sintering of glasses by a viscous flow mechanism, crystallization should be avoided during sintering, since once crystallization starts the viscosity of glass increases rapidly and sintering will be interrupted.

The purpose of this study is to investigate the combined effects of both B_2O_3 and TiO_2 addition on sintering and crystallization behaviors of β-spodumene glass-ceramics. In detail, the focus of this research is not only to enhance sintering, but also to decrease the crystallization temperature of β-spodumene glass-ceramics by addition of both B_2O_3 and TiO_2 for engineering applications such as composite fabrication.

2 Experimental Procedures

High purity powders (Li_2CO_3, Al_2O_3, SiO_2, B_2O_3 and TiO_2), were used to produce β-spodumene glass-ceramics. The chemical compositions of each glass are listed in Table 1. B_2O_3 (3 wt%) and TiO_2 (3 wt%) were added to the stoichiometric com-

Table 1. Compositions of glasses formed for present study

Glasses	*Components*				
	Li_2O (wt%)	Al_2O_3 (wt%)	SiO_2 (wt%)	B_2O_3 (wt%)	TiO_2 (wt%)
LA4S	8·02	27·40	64·58	—	—
LA4SB	7·80	26·59	62·69	2·92	—
LA4ST	7·72	26·34	62·09	—	3.85
LA4SBT	7·50	25·60	60·35	2·80	3·75

position of β-spodumene. The chemicals were well mixed by zirconia-ball milling (YTZ Zirconia-Ball Media, Tosoh USA Inc., Atlanta, GA). The glasses were prepared in the 50 cm^3 alumina crucibles (Coors Ceramics Co., Golden, CO) using an electrical resistance furnace (DT-31-HT, Deltech Inc., Denver, CO) in an air atmosphere. To homogenize the melt the mixture of chemicals were held at 1600°C for 3 h. The alumina crucible with the glass melt was removed from the furnace and quenched in distilled water to obtain a clear glass. Pouring the glass melt from the crucible was impossible due to the high viscosity and difficulty in temperature control. Glass fragments were hand ground after being well dried in the oven. The ground powders were screened by a 325-mesh sieve and then ball-milled in a rotating milling machine with the same zirconia balls in methyl alcohol. After 6 h milling with a ball-milling speed of approximately 180 rpm the size of the glass particles ranged from 5 to 10 μm. No zirconia contamination was detected by using energy dispersive X-ray spectroscopy (EDS: TN-5500, Noran Co., Middleton, WI) analysis. Crystallinity and crystallization temperatures of these glass powders were investigated by using wide-angle X-ray diffraction (XRD: Nicolet Stoe Transmission/Bragg-Brentano, Stoe Co., Germany) and differential thermal analysis (DTA: Perkin-Elmer DTA 1700, Norwalk, CT), respectively. The DTA measurements were performed using 65 mg of glass powders in an alumina crucible in an air atmosphere with heating rates of 3, 5, 10, 20, 40 and 80°C min from 500 to 1200°C. The DTA results were further analyzed to obtain the crystallization mode and the activation energy values for crystallization of each glass using various methods: Kissinger,[23] modified Kissinger,[24] Ozawa,[25] and Augis-Bennett.[26] The reason that all of these methods were used for present study is to obtain more accurate activation energy values for the glasses. The ball-milled powders mixed with organic binder (mixture of poly(vinyl butyral) and acetone) were cold pressed in a 6·4 mm diameter cylindrical steel die under a pressure of 20·7 MPa. These small pellets were sintered and crystallized in an electrical resistance furnace in an air atmosphere at the temperatures pre-selected from DTA measurements for different periods to obtain the optimum heat-treatment conditions. Sintering and crystallization of heat-treated samples were examined by scanning electron microscopy (SEM: Jeol SEM 35-C, Jeol, Japan) and XRD, respectively.

3 Results and Discussion

The XRD results for the four different glasses showed clear non-crystallinity. DTA result from LA4S glass is shown in Fig. 1. The other glasses showed similar DTA results. LA4ST and LA4SBT glasses, however, showed sharper crystallization exothermic peaks than LA4S and LA4SB glasses. The DTA results were analyzed primarily using the Kissinger equation:[23]

$$\ln (\phi/T_p^2) = -E_{ck}/RT_p + \text{const.} \qquad (1)$$

where ϕ is the DTA heating rate; T_p is the crystallization peak temperature; E_{ck} is the activation energy for crystallization estimated by the Kissinger method; and R is the gas constant. The Kissinger plots according to eqn (1) for these four glasses appear in Fig. 2. LA4SBT has the lowest activation energy value for crystallization, whereas LA4S has the highest. Even though the finely distributed precursor nuclei of $Al_2Ti_2O_7$ or separated TiO_2-rich phase in LA4ST glass can make subsequent crystallization easier and reduce the activa-

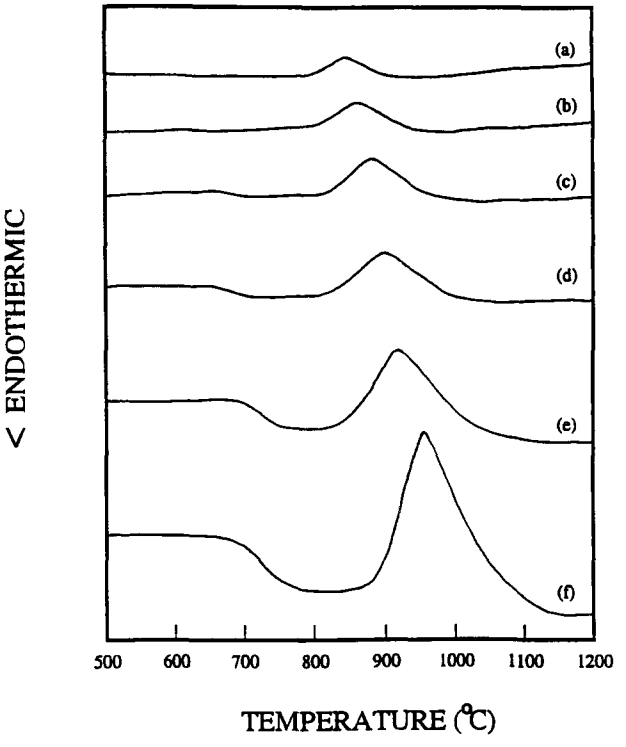

Fig. 1. The differential thermal analysis (DTA) curves for the LA4S glass with heating rates of (a) 3, (b) 5, (c) 10, (d) 20, (e) 40 and (f) 80°C/min.

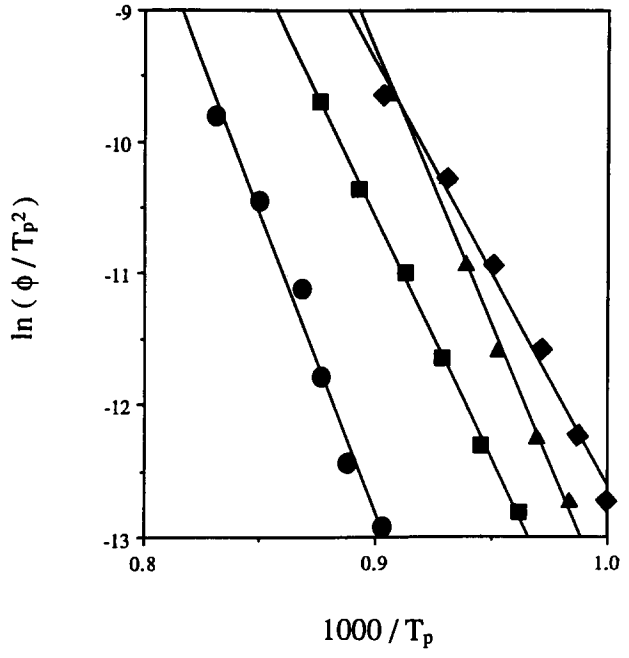

Fig. 2. The Kissinger plots for the glasses of ●, LA4S; ■, LA4SB; ▲, LA4ST and ♦, LA4SBT.

tion energy value, the B_2O_3 addition would be more effective in reducing the activation energy value by decreasing the viscosity of the glass.[8–15] This decreased viscosity can help crystallization, since crystallization is a diffusion-dominated phenomenon. LA4SBT has both the TiO_2 and B_2O_3 effects and shows the lowest activation energy value. Matusita & Sakka[24] mentioned that the Kissinger equation is valid only when the number of nuclei is fixed during crystal growth. If most nuclei are formed during the DTA run, the activation energy values from the Kissinger

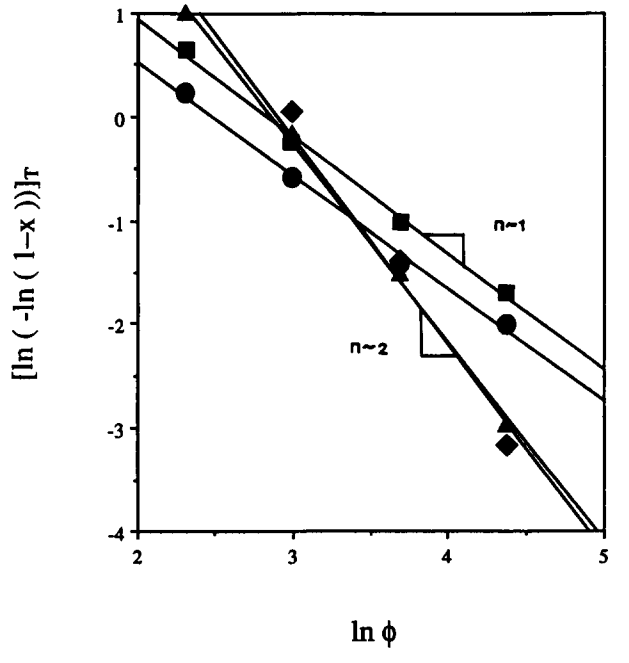

Fig. 3. The Ozawa plots for the glasses of ●, LA4S at 890°C; ■, LA4SB at 840°C; ▲, LA4ST at 810°C and ♦, LA4SBT at 800°C. Avrami parameter n = 1 for LA4S and LA4SB, and 2 for LA4ST and LA4SBT.

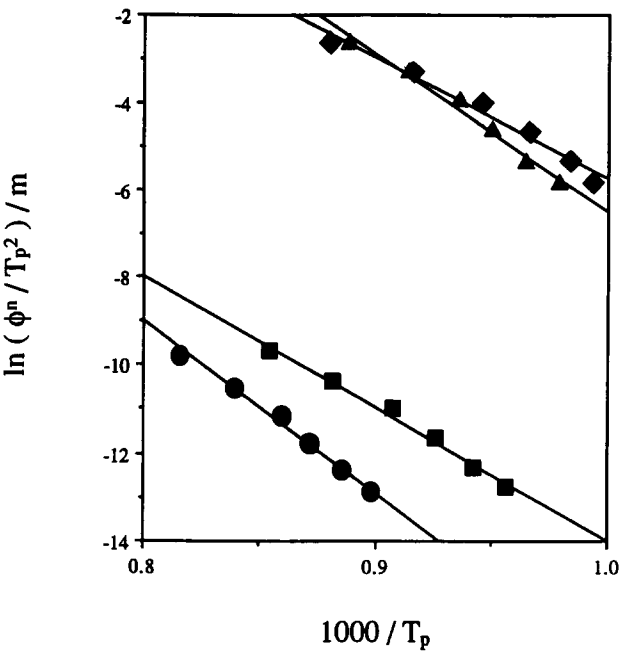

Fig. 4. The modified Kissinger plots the glasses of ●, LA4S; ■, LA4SB; ▲, LA4ST and ♦, LA4SBT. Avrami parameter n = 1 for LA4S and LA4SB, and 2 for LA4ST and LA4SBT. Dimensionality of crystal growth m = 1 for LA4S and LA4SB, and 2 for LA4ST and LA4SBT.

equation are incorrect. They suggested a modified form of the Kissinger equation:

$$\ln (\phi^n/T_p^2) = -mE_{cmk}/RT_p + \text{const.} \qquad (2)$$

where E_{cmk} indicates the correct activation energy for crystallization via the modified Kissinger method, n is an Avrami constant, and m is the dimensionality of crystal growth. When surface crystallization dominates, n = 1, and when bulk crystallization dominates, n = 3. The value of m is related to n as: $m = n$ when crystallization at different heating rates occurs on a fixed number of nuclei (in other words the number of nuclei is constant during the DTA runs at different values of ϕ); $m = n - 1$ when nucleation occurs during the DTA runs. In addition, when surface nucleation dominates, $m = n$ = 1 and eqn (2) essentially reduces to eqn (1). This means that when surface crystallization dominates, the activation energy values from the Kissinger equation (E_{ck}) will become the correct values, that is $E_{ck} = E_{cmk}$.

The values of the Avrami constant can be determined by the Ozawa equation:[25]

$$[\mathrm{d} \ln (-\ln(1 - x))/\mathrm{d} \ln \phi]_T = -n \qquad (3)$$

where x is the volume fraction crystallized at a fixed temperature T when heated at ϕ. That is, x is the ratio of the partial area at T to the total area of the crystallization exotherm. Ozawa plots from eqn (3) shown in Fig. 3 indicate that surface crystallization dominates both in the LA4S and LA4SB (n = ~1) glasses, and surface and bulk crystallization occurs simultaneously both in LA4ST and LA4SBT (n = ~2). Thus, m values

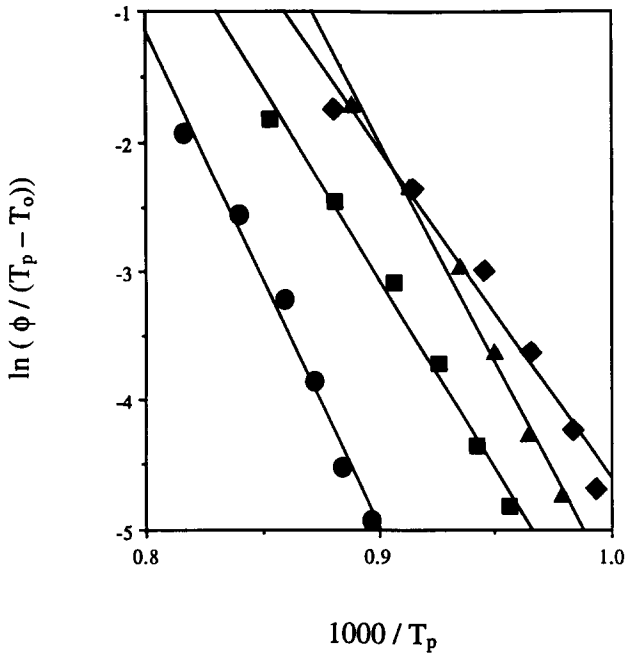

Fig. 5. The Augis–Bennett plots the glasses of ●, LA4S; ■, LA4SB; ▲, LA4ST and ♦, A4SBT.

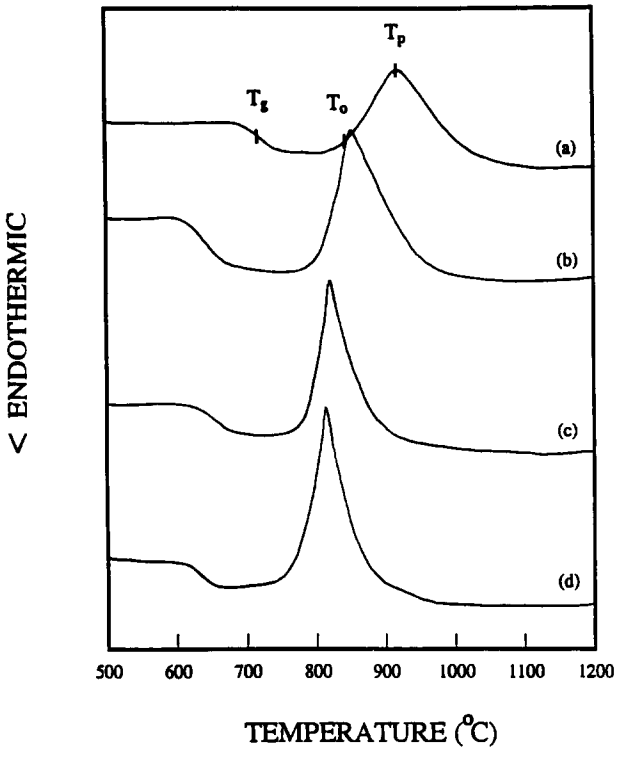

Fig. 6. The differential thermal analysis (DTA) curves for (a) LA4S, (b) LA4SB, (c) LA4ST and (d) LA4SBT glasses with heating rates of 40°C/min.

for LA4S and LA4SB become 1 because of the dominance of surface crystallization and that of LA4ST and LA4SBT becomes 2 due to the pre-existing nuclei of $Al_2Ti_2O_7$ or separated TiO_2-rich phases. The modified Kissinger plots for the four glasses according to eqn (2) are presented in Fig. 4. The modified Kissinger plots for LA4S and LA4SB are identical to the Kissinger plots since $m = n = 1$. To further confirm the accuracy of the above results for activation energy values, the following Augis & Bennett[26] equation can be applied:

$$\ln (\phi/(T_p - T_0)) = -E_{cab}/RT_p + \text{const.} \quad (4)$$

where T_0 is the temperature from which sample was heated with constant heating rate and is 400°C for the present study. E_{cab}, which indicates the activation energy for crystallization via the Augis & Bennett method, can be calculated from the plots of In $(\phi/(T_p - T_0))$ versus $1/T_p$, as shown in Fig. 5. All activation energy values from this method are in good agreement with those from the other methods. All of these DTA results are summarized in Table 2.

Figure 6 presents DTA data for the four glasses with a heating rate of 40°C/min. In glass-ceramic systems the viscous flow of the glass above the glass transition temperature (T_g) is the sintering mechanism. Sintering by glass flow will be hindered once crystallization is initiated. Thus, to obtain a good sintering a glass should be sintered near but below the crystallization temperature. If one glass has T_g and T_o (crystallization onset temperature) values which are too close to each other, then the glass can not be fully densified by sintering below T_o, since it is highly possible that crystallization may occur before sintering ends. Thus, the glass-ceramic which has large temperature range between T_g and T_0 has the potential to result in a well-sintered product. T_g, T_0, T_p, and $T_0 - T_g$ for the four glasses are listed in Table 3. B_2O_3 addition to

Table 2. Summary of DTA results of glasses formed for present study

Properties	*Glasses*			
	LA4S	*LA4SB*	*LA4ST*	*LA4SBT*
Avrami parameter (n)	1	1	2	2
Dimensionality of crystal growth (m)	1	1	2	2
E_{ck} (kJ/mol) (Kissinger)	325	251	290	219
E_{cmk} (kJ/mol) (modied Kissinger)	325	251	299	228
E_{cab}(kJ/mol) (Augis–Bennett)	318	245	283	212

Table 3. Summary of temperature values from DTA results of glasses formed for present study

Glasses	*Temperatures or temperature ranges (°C)*			
	T_g *(glass transition)*	T_0 *(crystal-lization onset)*	T_p *(crystal-lization peak)*	T_0–T_g
LA4S	715	835	918	120
LA4SB	658	784	862	126
LA4ST	662	770	821	108
LA4SBT	640	761	819	121

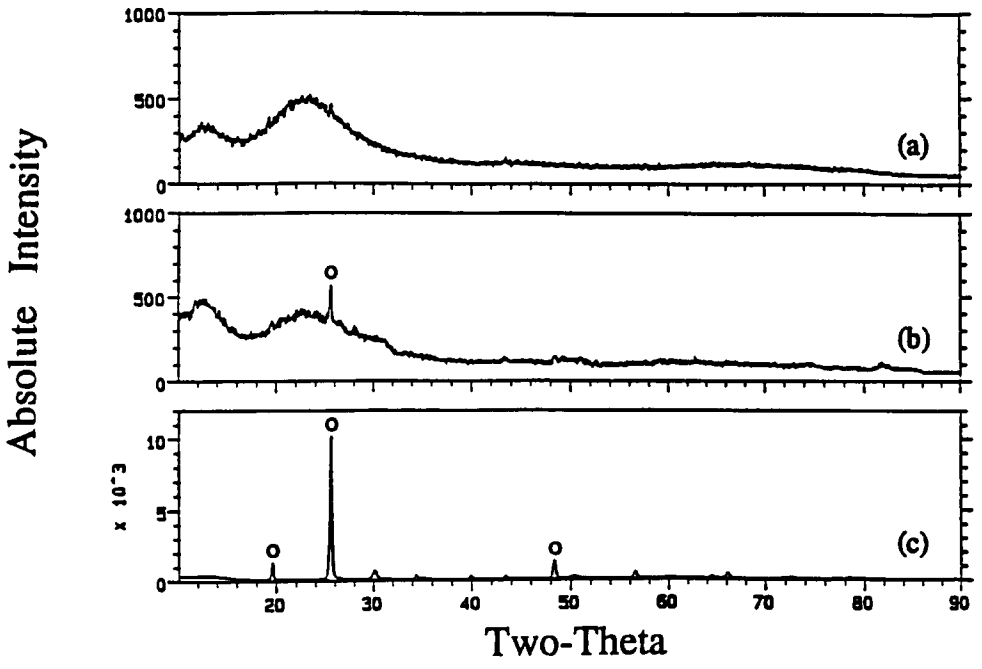

Fig. 7. The X-ray diffraction (XRD) patterns showing the initiation of crystallization of β-spodumene phase (○) for the LA4SB glass sintered at 715°C for (a) 2, (b) 4 and (c) 6 h.

LA4S increased $T_o - T_g$ values by suppressing the T_g to a lower temperature, since B_2O_3 can decrease the viscosity of this glass even though it can act as a network former. The effect of TiO_2 addition decreased T_p of the LA4S glass by 99°C, most probably due to the existence of precursor nuclei of $Al_2Ti_2O_7$ or separated TiO_2-rich phases which subsequently acted as crystallization sites of the β-spodumene phase.[1,17,18,21,22] The effect of TiO_2 addition may be poor sintering of these glass powders due to the rapid crystallization at low temperatures. The small temperature range between T_g and T_0 resulting from lower T_0 of LA4ST supports this idea and the poor sintering of LA4ST was observed from sintering experiments. The B_2O_3 addition can mitigate this problem. LA4SB and LA4SBT glasses have larger $T_0 - T_g$ ranges than LA4ST and these B_2O_3 modified glasses are expected to sinter more readily. The XRD patterns for LA4SB sintered at 715°C for 2,4 and 6 h are shown in Fig. 7. The 6-h sintering of LA4SB at 715°C resulted in nearly total crystallization of the β-spodumene phase. Figure 8 shows the XRD patterns for LA4SBT sintered at 700°C for 0·5, 1 and 2 h. This figure indicates that crystallization of β-spodumene phase for this system starts after approximately 1 h sintering at 700°C. The effect of the TiO_2 addition is evident in that LA4SBT crystallizes faster than LA4SB even at lower temperatures. Figure 9 shows XRD patterns of (a) LA4SB sintered at 715°C for 2 h and crystallized at 865°C for 2h, and (b) LA4SBT sintered at 700°C for 1 h and crystallized at 830°C for 2 h. Both XRD patterns clearly show the

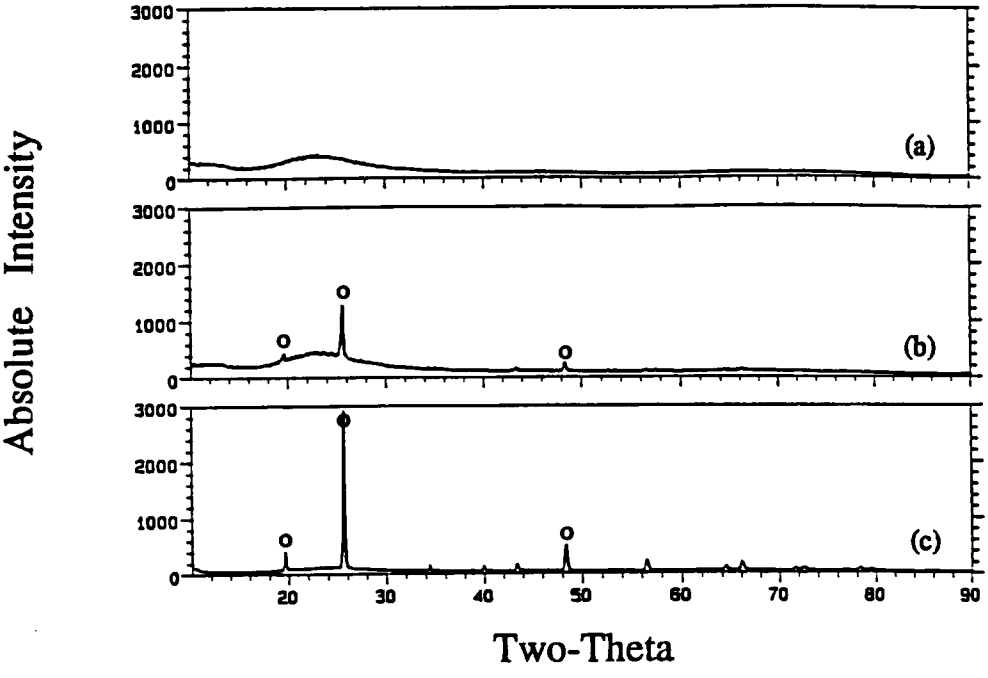

Fig. 8. The X-ray diffraction (XRD) patterns showing the initiation of crystallization of β-spodumene phase (○) for the LA4SBT glass sintered at 690°C for (a) 0.5, (b) 1 and (c) 2 h.

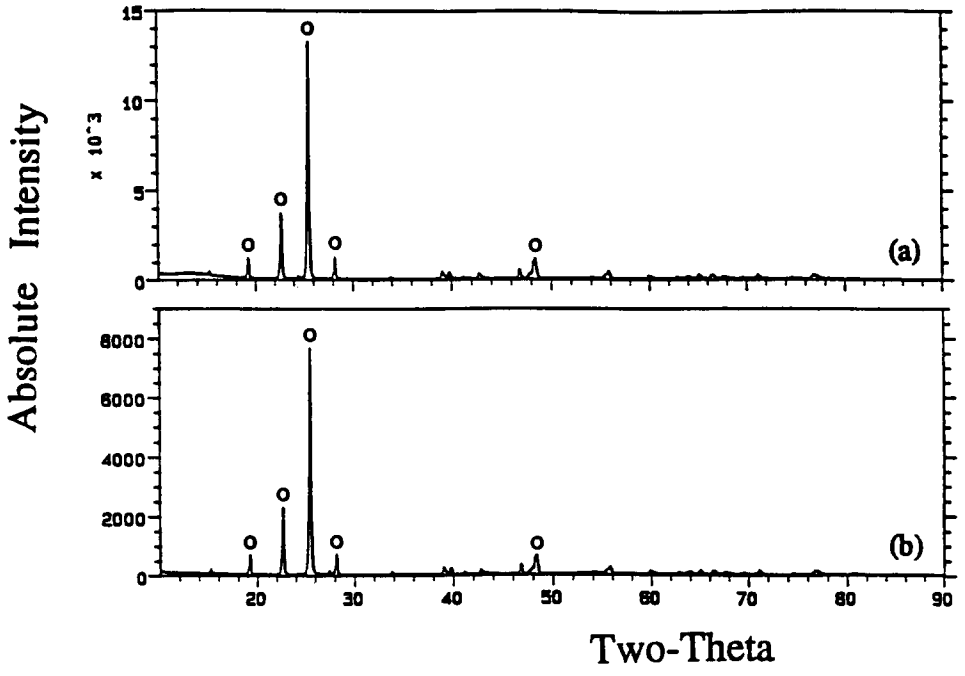

Fig. 9. The X-ray diffraction (XRD) patterns showing the formation of β-spodumene phase (○) for (a) LA4SB glass-ceramic sintered at 715°C for 2 h and crystallized at 865°C for 2 h and (b) LA4SBT glass-ceramic sintered at 690°C for 1 h and crystallized at 830°C for 2 h.

major peaks from the β-spodumene phase. SEM photographs for (a) LA4SB sintered at 730°C for 2 h and crystallized at 865°C for 2h and (b) LA4SBT sintered at 700°C for 1 h and crystallized at 830°C for 2 h are shown in Fig. 10. Both of the samples show about the same degree of sintering and less than 1-μm-sized β-spodumene crystallites within the sintered granules.

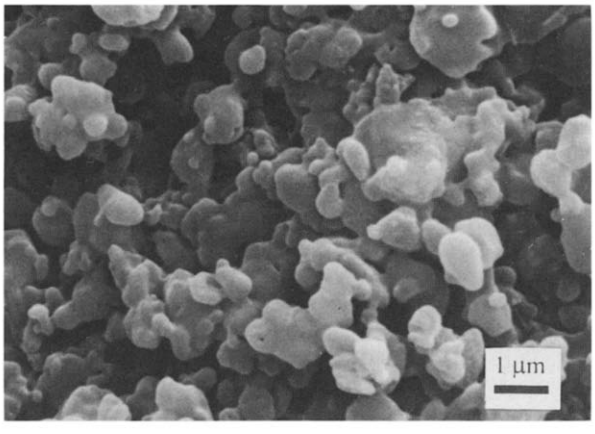

(a)

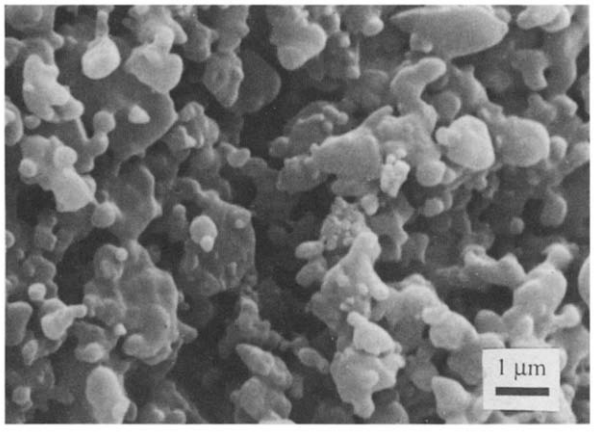

(b)

Fig. 10. The scanning electron micrographs for (a) LA4SB glass-ceramic sintered at 715°C for 2 h and crystallized at 865°C for 2 h and (b) LA4SBT glass-ceramic sintered at 690°C for 1 h and crystallized at 830°C for 2 h.

4 Conclusions

(1) From the DTA results LA4S and LA4SB showed surface crystallization (Avrami parameter of 1) and LA4ST and LA4SBT which have precursor nuclei of $Al_2Ti_2O_7$ or separated TiO_2-rich phases, showed mixed surface and bulk crystallization (Avrami parameter of 2).

(2) From the DTA results the activation energy values for crystallization of LA4S, LA4SB, LA4ST and LA4SBT were respectively determined as 322 ± 4, 248 ± 3, 291 ± 8 and 220 ± 8 kJ/mol via Kissinger, modified Kissinger and Augis–Bennett methods. This result implies that both B_2O_3 and TiO_2 can make crystallization easier by reducing the viscosity of glass by B_2O_3 and by forming the precursor nuclei for crystallization by TiO_2.

(3) From the DTA measurements the crystallization peak temperature (T_p) values for LA4S, LA4SB, LA4STand LA4SBT with a DTA heating rate of 40°C/min were determined as 918, 862, 821 and 819°C, respectively. The T_p value of LA4SBT is the lowest since it has lower viscosity by B_2O_3 addition and precursor nuclei by TiO_2 addition.

(4) The XRD pattern for the LA4SB sintered at 715°C showed the initiation of crystallization of β-spodumene phase at a 4 h heat

treatment, whereas that for LA4SBT sintered at 690°C indicated the initiation of crystallization of β-spodumene phase at a 1 h treatment.

(5) The SEM for the LA4SB and LA4S glass-ceramics showed approximately the same degree of sintering.

Acknowledgments

The authors wish to thank Dr Kyoungho Lee at Virginia Polytechnic Institute for many helpful discussions. The authors also acknowledge Mr Yonsoo Sung, Professor Eric E. Hellstrom and Professor John H. Perepezko at University of Wisconsin–Madison for providing access to their experimental facilities. Finally, the authors would like to express their appreciation to the reviewers and Dr R. Nathan Katz for helpful comments.

References

1. Beall, G. H. & Duke, D. A., Glass-ceramic technology. In *Glass Science and Technology, Vol. 1*, ed. D. R. Uhlmann & N. J. Kreidl. Academic Press, New York, 1983, pp. 403–45.
2. Marshall, D. B. & Evans, A. G., Fracture mechanism in ceramic–fiber/ceramic–matrix composites. *J. Am. Ceram. Soc.*, **68** (1985) 225–31.
3. Prewo, K. M., Brennan, J. J. & Layden, G. K., Fiber-reinforced glasses and glass-ceramics for high performance applications. *Am. Ceram. Soc. Bull.*, **65** (1986) 305–22.
4. Bishoff, E., Ruhle, M., Sbaizero, O. & Evans, A. G., Microstructural studies of the interfacial zone of a SiC-fiber-reinforced lithium aluminum silicate glass-ceramic. *J. Am. Ceram. Soc.*, **72** (1989) 741–5.
5. Bonney, L. A. & Cooper, R. F., Reaction-layer interfaces in SiC-fiber-reinforced glass-ceramics: a high-resolution scanning transmission electron microscopy analysis. *J. Am. Ceram. Soc.*, **73** (1990) 2916–21.
6. Homeny, J., VanValzah, J. R. & Kelley, M. A., Interfacial characterization of silicon carbide fiber/lithia–alumina–silica glass–ceramic matrix composites. *J. Am. Ceram. Soc.*, **73** (1990) 2054–9.
7. Tummala, R. R., Ceramic and glass-ceramic packaging in the 1990s. *J. Am. Ceram. Soc.*, **74** (1991) 895–908.
8. Knickerbocker, S. H., Kumar, A. H. & Herron, L. W., Cordierite glass-ceramics for multilayer ceramic packaging. *Am. Ceram. Soc. Bull.*, **72** (1993) 90–5.
9. Doremus, R. H., *Glass Science*. Wiley, New York, 1973, p. 75.
10. Grossman, D. G., Glass-ceramic applications. In *Advances in Ceramics*, Vol. 4, *Nucleation and Crystallization in Glasses*, ed. J. H. Simmons, D. R. Uhlmann & G. H. Beall. American Ceramic Society, Columbus, OH, 1982, pp. 249-60.
11. Rabinovich, E. M., Review: preparation of glass by sintering. *J. Mater. Sci.*, **20** (1985) 4259–97.
12. Helgesson, C. I., Properties of cordierite glass-ceramics produced by sintering and crystallization of glass powder. In *Science of Ceramics*, Vol. 8. British Ceramic Society, Stoke-on-Trent, UK, 1976, pp. 347–61.
13. Giess, E. A., Fletcher, J. P. & Herron, L. W., Isothermal sintering of cordierite-type glass powders. *J. Am. Ceram. Soc.*, **67** (1984) 549–52.
14. Rabinovich, E. M., Cordierite glass-ceramics produced by sintering. In *Advances in Ceramics*, Vol. 4, *Nucleation and Crystallization in Glasses*, ed. J. H. Simmons, D. R. Uhlmann & G. H. Beall. American Ceramic Society, Columbus, OH, 1982, pp. 327–33.
15. Knickerbocker, S., Tuzzolo, M. R. & Lawhorne, S., Sinterable β-spodumene glass-ceramics. *J. Am. Ceram. Soc.*, **72** (1989) 1873–9.
16. Strinad, Z., Glass-ceramic materials. In *Glass Science and Technology*, Vol. 8, Elsevier Science, New York, 1986.
17. Barry, T. I., Clinton, D., Lay, L. A., Mercer, R. A. & Miller, R. P., The crystallization of glasses based on the eutectic compositions in the system Li_2O–Al_2O_3–SiO_2, Part I. *J. Mater Sci.*, **4** (1969) 596–612.
18. Doherty, P. E., Lee, D. W. & Davis, R. S., Direct observation of the crystallization of Li_2O–Al_2O_3–SiO_2 glasses containing TiO_2. *J. Am. Ceram. Soc.*, **55** (1970) 77–81.
19. Maier, V. & Muller, G., Mechanism of oxide nucleation in lithium aluminosilicate glass-ceramics. *J. Am. Ceram. Soc.*, **70** (1987) C176–8.
20. Hsu, J. & Spyer, R. F., Comparison of the effects of titania and tantalium oxide nucleating agents on the crystallization of Li_2O–Al_2O_3–$6SiO_2$ glass. *J. Am. Ceram. Soc.*, **72** (1989) 2334–41.
21. Buzhinskii, I. M., Sabaeva, E. I. & Khomyakov, A. N., In *The Glass State*, Vol. 1, *Catalyzed Crystallization of Glass*, Izd. Akad. Nauk SSSR, Moscow–Leningrad, 1963. English translation: *The Structure of Glass*, Vol. 3, Consultants Bureau, New York, 1964, pp. 133–45.
22. Alekseeva, A. G., Vertsner, V. N. & Kondrat'ev, Y. N., *Dokl. Akad. Nauk SSSR*, **154** (1964) 178–80.
23. Kissinger, H. E., Variation of peak temperature with heating rate in differential thermal analysis. *J. Res. Natl. Bur. Stand. (U.S.)*, **57** (1956) 217–21.
24. Matusita, K. & Sakka, S., Kinetic study on crystallization of glass by differential thermal analysis—criterion on application of Kissinger Plot. *J. Non-Cryst. Solids*, **38–39** (1980) 741–6.
25. Ozawa, T., Kinetics of non-isothermal crystallization. *Polymer*, **12** (1971) 150–8.
26. Augis, J. A. & Bennett, J. E., Calculation of the Avrami parameters for heterogeneous solid-state reactions using a modification of the Kissinger method. *J. Therm. Anal.*, **13** (1978) 283–92.